The Role of Hole Transport between Dyes in Solid State Dye Sensitized Solar Cells

Davide Moia,[1] Ute B. Cappel,[2] Tomas Leijtens,[3] Xiaoe Li,[2] Andrew M. Telford,[1] Henry J. Snaith,[3] Brian C. O'Regan,[2] Jenny Nelson,[1] and Piers R. F. Barnes[1*]*

1. Blackett Laboratory, Imperial College London, London SW7 2AZ, UK
2. Department of Chemistry, Imperial College London, London SW7 2AZ, UK
3. Clarendon Laboratory, University of Oxford, OX1 3PU, UK
*davide.moia11@imperial.ac.uk; piers.barnes@imperial.ac.uk

Abstract

In dye-sensitized solar cells (DSSCs) photo-generated positive charges are normally considered to be carried away from the dyes by a separate phase of hole transporting material (HTM). We show that there can also be significant transport within the dye monolayer itself before the hole reaches the HTM. We quantify the fraction of dye regeneration in solid state DSSCs that can be attributed to this process. By using cyclic voltammetry and transient anisotropy spectroscopy we demonstrate that the rate of inter-dye hole transport is prevented both on micrometer and nanometer length scales by reducing the dye loading on the TiO_2 surface. The dye regeneration yield is quantified for films with high and low dye loadings (with and without hole percolation in the dye monolayer) infiltrated with varying levels of HTM. Inter-dye hole transport can account for >50% of the overall dye regeneration with low HTM pore filling. This is reduced to about 5% when the infiltration of the HTM in the pores is optimized in 2µm thick films. Finally, we use hole transport in the dye monolayer to characterize the spatial distribution of the HTM phase in the pores of the dyed mesoporous TiO_2.

Introduction

The dye sensitized solar cell (DSSC) is an alternative solar energy conversion technology based on low cost, low toxicity materials in the early stages of comercialization.[1] Liquid junction DSSCs include dye absorbers sensitizing a nanoparticulate film of titanium dioxide which is then infiltrated with a liquid solvent containing a redox couple. Under operating conditions, light is absorbed by the dye molecules on the surface of the TiO_2. Photoexcited electrons are then injected into and transported through the TiO_2 scaffold, while the redox couple is used to transfer the holes from the dyes to the counter electrode of the cell.[2] Among many factors, the attraction to DSSCs is due to their wide selection of sensitization colors and potential for building integration. However, commercialization of the technology has faced some important issues. Above all, the use of a liquid electrolyte raises limitations on the manufacturing options to provide good sealing of the cell. To overcome this issue, the solid state DSSC concept has been presented, where the liquid electrolyte is replaced by a solid state hole transporting material, typically an organic semiconductor deposited from solution on top of the mesostructure.[3] In this architecture, the photogenerated holes remaining on the dye molecules following electron injection into the TiO_2 are transferred to the hole transporting material (HTM). This process is referred to as regeneration of the photo-oxidized dye. High regeneration yield is required in order to achieve good charge collection efficiency. For this reason, full coverage of the dye monolayer by the HTM is desirable.

Solution processing of the HTM on the mesostructure of TiO_2 generally results in limited pore filling (pore filling is defined as the pore volume fraction occupied by the HTM). As examples, values up to about 85% have been reported from reflectance measurements for 2.6 µm thick optimized devices in which the indolene dye D102 was used as the sensitizer and 2,2',7,7'-Tetrakis(N,N -di-p -methoxyphenylamino)-9,9'- spirobifluorene (spiro OMeTAD) as HTM.[4] However, the relevant figure of merit in regard to dye regeneration is pore coverage, which we define as the fraction of dyed TiO_2

surface which is in contact with the HTM phase. This parameter has been qualitatively discussed but, to date, it has not been quantified. From electrochemical studies of TiO_2 mesostructures sensitized with the dye D131 and infiltrated with the hole conductors spiro OMeTAD and P3HT we have shown that, when pore filling is increased, surface coverage also increases.[Unpublished data] However, this study suggested that, for 1.8 µm thick devices under optimized pore filling conditions, surface coverage does not reach 100%. This observation implies that, in commonly fabricated solid state DSSCs, a fraction of the dyes are not in contact with the HTM phase. Therefore, under operating conditions, a significant fraction of holes are potentially trapped on dye molecules resulting in higher recombination and suboptimal charge collection efficiency.

Photoinduced absorption (PIA) and transient absorption spectroscopy (TAS) have been used by research groups to investigate and quantify the regeneration performance of solid state DSSCs.[5,6,7,8,9] Some of these studies have shown that, under optimized conditions and for different dyes and thickness of the TiO_2 layer, the dye regeneration yield of the device ranges between 0.9 and 1. This result suggests that either almost complete coverage of the dyed surface is achievable or transfer of holes between the dye molecules enables improved charge collection from dyes that are uncovered by the HTM.

Hole transport occurring between dyes anchored to nanocrystals in an inert electrolyte has been suggested and demonstrated. Electrochemical and spectroelectrochemical measurements of dye sensitized semiconducting and insulating mesostructures have shown diffusion of charges through the monolayer of dyes corresponding to apparent diffusion coefficients between 10^{-10} and 10^{-7} cm^2 s^{-1}.[10,11,12,13,14] Hole diffusion can also be assessed by resolving the loss in optical absorption polarization in time of a population of holes generated with a polarized optical excitation pulse. This technique assumes that the absorption anisotropy of initially photogenerated holes is lost as the holes hop to neighboring molecules with differing orientations. Ardo and Meyer applied anisotropy spectroscopy to dyed mesoporous films and demonstrated the ability to monitor the process of charge diffusion at the nanoscale.[15] We have recently demonstrated that hole transport between dyes allows working DSSCs with no electrolyte and no hole transporting material.[16] Some studies have already argued that hole transport between dyes could happen in solid state devices and plays a role towards improved dye regeneration.[17,8,18,19,20,9] However, to our knowledge, no experimental evidence for this has been reported to date.

In this work, we use transient absorption and transient anisotropy spectroscopy to investigate solar cell structures where both dye coverage and pore filling by the HTM are varied (see figure 1). Thus two different concepts of coverage are considered: dye loading or coverage (fraction of the TiO_2 surface coated in dye molecules relative to complete coverage) and HTM coverage (the fraction of the sensitized TiO_2 surface coated by the HTM). We therefore address the following questions: is hole transport between dye molecules anchored to the nanocrystalline surface of TiO_2 occurring in solid state DSSCs? If so, does this phenomenon lead to an improvement in power conversion efficiency of the device? Furthermore, is the collection efficiency of current solid state devices still limited by poor surface coverage by the HTM? Would the design of dye molecules showing faster hole transport further improve the performance of this class of solar cells?

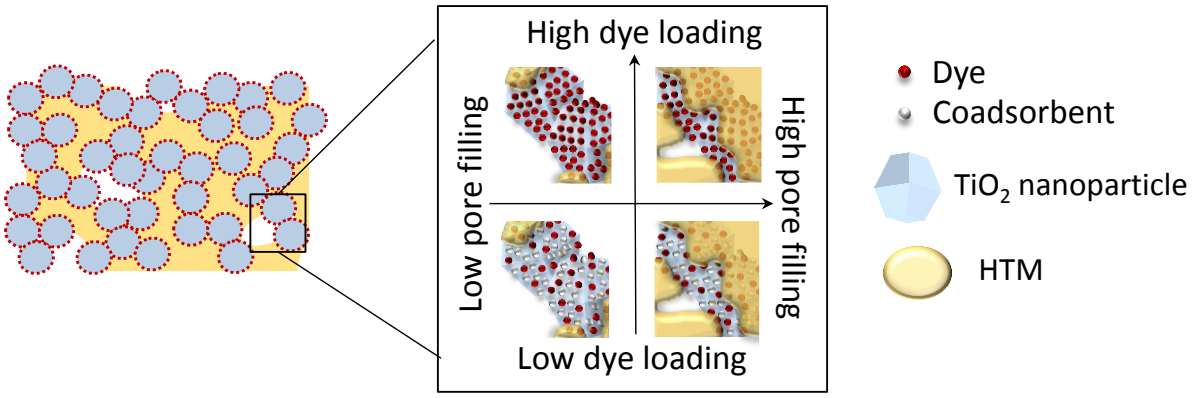

Figure 1. Solar cell structures investigated in this study: mesoporous films of TiO_2 have been sensitized with dye solution containing an inert, colorless coadsorbent in order to obtain different dye loading conditions. The dyed film was then infiltrated with a hole transporting material (HTM). This was done via spin coating of solutions containing different concentrations of the HTM in order to control the pore filling.

Method

The sample fabrication procedure, the experimental details on dye loading quantification, electrochemical measurements and calculation of the pore filling fraction can be found in section 1 of the Supporting Information.

Transient absorption measurements: transient spectroscopy was carried out with an extension of the setup described in reference [21]. A Nd:YAG pumped OPO (Opotek Opolette 355) was used as pump with wavelength 450 nm for D131 samples. The repetition rate was 10 Hz for the study of regeneration in solid state DSSCs and 20Hz for percolation experiments. Fluence was kept between 6 and 10 µJ cm^{-2}. Samples were placed perpendicularly to the pump beam, which was directed from the laser output through a beam-guide, and slightly offset (about 30°) with respect to the main optical axis defined by the probe beam. A 100W quartz halogen lamp (Bentham IL1) driven by constant current power supply (Bentham 605) was used as probe light source in the system. Neutral density and long pass filters were used to attenuate the intensity of the probe and to limit its spectral range to wavelengths above the absorption window of the dye. After the sample, the probe beam was passed through a monochromator where the probe wavelength was selected before reaching an infrared detector. The electrical signal from the detector was amplified via a Costronics preamplifier and amplifier and recorded with an oscilloscope (Tektronix TDS 1012). The amplifier also measured the background level which was used to calculate the variation in optical density upon laser excitation, ΔOD, using the formula $\Delta OD(t) = -\log_{10}(1 + V(t)/V_{BG}) \approx - V(t)/(V_{BG} \times 2.3)$ where $V(t)$ is the transient signal and V_{BG} the background level. In some cases, recombination of charges generated by a laser pulse in the sample under study was not complete before the next pulse. This implies that a background concentration of charges was present in some of the measurements. The presence of a background concentration of holes during the experiment will increase their rate of recombination with the electrons in the TiO_2. Our analysis of hole transfer between dyes and between dye and HTM phases shows that no significant recombination occurs in the 1µs - 100 µs timescale for all samples. This implies that the presence of the background charge concentration does not influence the values of regeneration yield (η_{reg}) calculated in our analysis (η_{reg} is evaluated within 2 µs <t< 40 µs, see eq. 3 below). We also note that the experiment was carried out in the absence of a bias light and so will not give an accurate description of the regeneration yield at 1 sun. However, since regeneration occurs predominantly at time scales faster than 1 µs and at 1 sun electron-oxidized dye recombination occurs on timescales > 1 µs (see figure 4 in reference [16]), we expect the trend we present to reflect the behavior of devices even under working conditions. Table

1 shows the values of the extinction coefficients used in this study. 1000 and 1500 nm were used as probe wavelengths. The absorption of electrons in the conduction band of the TiO_2 was neglected in all cases (their extinction coefficient in this wavelength range is expected to be lower than 1500 M^{-1} cm^{-1} [22,23]).

Table 1. List of the values of extinction coefficient in M^{-1} cm^{-1} used in this study for D131 and spiro OMeTAD cations.

Probe wavelength	D131 cation	Spiro OMeTAD cation
1000 nm	20573 [a]	3000 [c]
1500 nm	0 (<1500 [b])	30000 [c]

The letter in square brackets refers to the method used to extract the value according to the following legend: [a] taken from spectroelectrochemistry measurements in 0.1 TBAP acetonitrile (see section 2 in the supporting information); [b] this value has been calculated by comparing the ΔOD measured at the relevant wavelength and at 1000 nm for dye sensitized films in air, given the value of the extinction coefficient measured at 1000 nm in 0.1 TBAP acetonitrile using method [a]; [c] taken from reference [24].

Transient absorption data have been processed by assigning the observed signals to the contribution from holes on the dyes or in the spiro OMeTAD phase. We define the hole density per unit geometric area in species *i* as $p_i(t) = \int_0^d p_i(z,t)dz$ (cm^{-2}) where *z* corresponds to the axis perpendicular to the plane (*z* = 0) defined by the sample's substrate, *d* is the thickness of the film in cm and $p_i(z,t)$ is the hole density per unit volume along the thickness of the film (cm^{-3}). For D131 sensitized samples, Δ*OD* measured at 1000 and 1500 nm can be expressed as a function of $p_{D131}(t)$ and $p_{spiro}(t)$ by using the following model:

$$\begin{bmatrix} \Delta OD_{1000nm}(t) \\ \Delta OD_{1500nm}(t) \end{bmatrix} = \begin{bmatrix} \varepsilon_{D131+,1000nm} & \varepsilon_{spiro+,1000nm} \\ \varepsilon_{D131+,1500nm} & \varepsilon_{D131+,1500nm} \end{bmatrix} \begin{bmatrix} p_{D131}(t) \\ p_{spiro}(t) \end{bmatrix} . \qquad \text{Eq.1}$$

In equation 1, $\varepsilon_{i,\lambda}$ is the extinction coefficient of species *i* at wavelength λ in M^{-1} cm^{-1}. From the time evolution of $p_{D131}(t)$ and $p_{spiro}(t)$ we calculate a time dependent dye regeneration yield as:

$$\eta_{reg}(t) = \frac{p_{spiro}(t)}{p_{spiro}(t) + p_{D131}(t)} \quad . \qquad \text{Eq. 2}$$

For all samples, the decay of the signals due to recombination of holes on the dyes or in the spiro OMeTAD were negligible up to few tens of microseconds. This model neglects any recombination happening at this or earlier timescales.

Dye regeneration yields were calculated by taking the average of $\Delta OD_{1000nm}(t)$ and of $\Delta OD_{1500nm}(t)$ between 2 and 40 µs: 2 µs is a conservative estimate of the rise time of the signal amplification electronics used for this measurement; the total concentration of holes in the film up to 40 µs was approximately constant for all samples (see figure 3a-d). These averaged values were used in equation 1 to find the averaged hole densities $\langle p_{D131} \rangle_{2\text{-}40\mu s}$ and $\langle p_{spiro} \rangle_{2\text{-}40\mu s}$. An estimate of the regeneration yield in the microsecond timescale was then calculated as:

$$\eta_{reg} = \frac{< p_{spiro} >_{2-40\mu s}}{< p_{spiro} >_{2-40\mu s} + < p_{D131} >_{2-40\mu s}} \qquad \text{Eq. 3}$$

Measurements of regeneration in solid state DSSCs were carried out within 8 hours after spin coating of the spiro OMeTAD.

For transient absorption anisotropy measurements, a similar setup to the one described above was used. The sample was placed at 45° with respect to the probe beam. The pump beam was passed through a Glan-Thompson polarizer (GTH10M-A from Thorlabs) before hitting the sample. The polarization of the pump was kept vertical with respect to the plane of the optical table and it was pointed towards the sample perpendicularly to the probe beam. A second polarizer (LPVIS050 from Thorlabs) was mounted before the monochromator to probe the vertical or horizontal polarization (parallel or perpendicular to the pump beam's polarization) of the transient optical signal transmitted through the sample or to measure the transient signal at the Magic angle. Δ*OD* was calculated as above for all conditions. The transient anisotropy *r*(t) was calculated from the measurements under vertical and horizontal polarization of the probe beam ($\Delta OD_V(t)$ and $\Delta OD_H(t)$) as:[25]

$$r(t) = \frac{\Delta OD_V(t) - \Delta OD_H(t)}{\Delta OD_V(t) + 2\Delta OD_H(t)} \qquad \text{Eq. 4}$$

For all the anisotropy measurements shown in this work, ΔOD_V has been calculated as the average of a measurement taken before the measurement of ΔOD_H and one taken after, to approximately compensate for any degradation of the film. The ratio of the amplitudes for the two ΔOD_V measurements was >0.9 for most measurements. For the percolation experiment, samples measured in air (20°C, 45% RH) were measured after being taken out of an acetonitrile solution where they had been stored in the dark for less than 5 hours after dyeing.

Results and discussion

Study of hole percolation at different scales

In this section we show that a hole percolation threshold is observed, both at the film thickness (µm) scale, and at the particle (10 nm) scale when the concentration of dyes on the TiO_2 surface is decreased. We also observe that hole diffusion is considerably faster in the presence of a solvent than in air. We demonstrate these effects using the indoline dye D131 since it is known to show hole hopping when anchored to TiO_2[13,19] and it is widely used in solid-state DSSCs showing among the highest IPCE peak values for this class of devices.[26] Also the absorption spectrum of the dye's oxidized state allows clear distinction from holes in spiro OMeTAD, the most widely used HTM in solid state DSSCs to date (see section 1 of the supporting information).

Attaining uniform dye loading is crucial for a meaningful investigation of percolation in the monolayer. For the case of films dyed with D131 only, sufficiently long dyeing time is needed to guarantee full coverage throughout the depth of the film, as also discussed in reference [27]. When the inert coadsorbent chenodeoxycholic acid (DCA) was included in the dye solution to obtain lower dye loading, we observe slow uptake kinetics of D131 on the surface due to the presence of the DCA. We also observe that dyeing of the bottom of the film occurs more quickly with DCA so that uniformity can be achieved with shorter dyeing times than without DCA as we show and discuss in section 3 of the supporting information.

Cyclic voltammetry of dye sensitized TiO_2 films showed a strong dependence on the dye loading. When decreasing the dye surface coverage of the TiO_2 film, the measured cyclic voltammogram showed a significant drop in the magnitude of the current density peak for similar scan rate conditions (Figure 2a). We evaluated the holes' apparent diffusion coefficient relative to each measurement by fitting a diffusion model which includes the effect of series resistance. The model used to analyse the data has been described in reference [19]. The values of the apparent diffusion

coefficient for D131 sensitized films are shown in Figure 2b as a function of fractional dye coverage. We note that for dye loading below ~30%, the value of the integrated current of the first cyclic voltammogram peak suggests that the number of dyes being oxidized is in the same order of magnitude as what is expected from an oxidation experiment for a monolayer of dyes (~1 dye per nm^2). This implies that the use of the term diffusion coefficient is no longer meaningful at low dye loading (below percolation). A percolation threshold is observed at dye loadings corresponding to about 40 to 60% of the maximum value of surface coverage measured in the experiment. The trend is consistent with previous reports on hole or electron diffusion on the surface of nanocrystals measured with electrochemistry.[11,12,28]

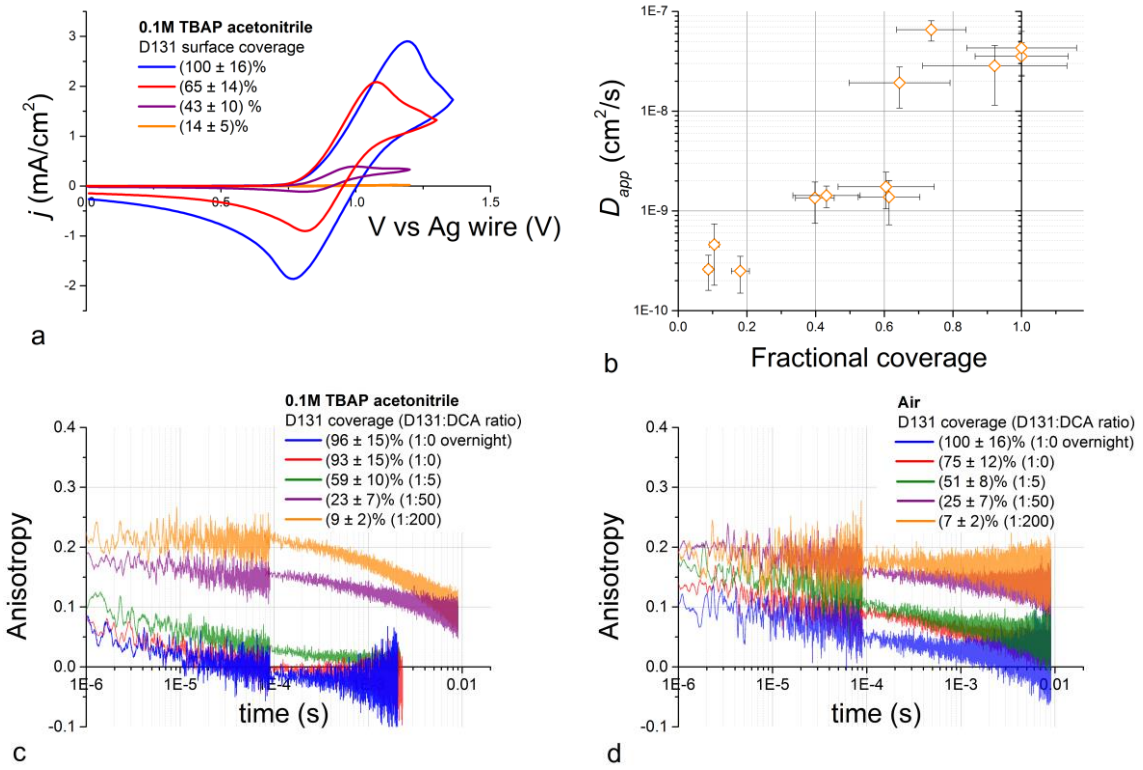

Figure 2. Analysis of hole percolation on D131 sensitized mesoporous TiO_2 using cyclic voltammetry and transient absorption anisotropy. (a) Cyclic voltammograms of D131:DCA sensitized mesoporous TiO_2 films on FTO glass measured at 0.2 V s^{-1} scan rate in 0.1M TBAP:acetonitrile, where *j* is the current density. (b) Apparent diffusion coefficient (D_{app}) plotted versus surface coverage, calculated as the dye loading of the sample divided by the maximum dye loading recorded for the experiment. (c, d) Transient anisotropy, $r(t)$, measurements of D131:DCA sensitized TiO_2 films immersed in 0.1M TBAP:acetonitrile (c) and in air (d). The samples were excited with polarized laser pulses at 450 nm (repetition rate 20 Hz).

Monitoring the changes in polarization of holes photogenerated via polarized laser pulses can also give insight into the diffusion of the charges within a dye monolayer. This information can be expressed by measuring the dye cation absorption anisotropy as described in the method section. Figure 2c-2d shows transient anisotropy measurements for D131:DCA sensitized TiO_2 films either in 0.1M TBAP dissolved in acetonitrile or in air. Loss in anisotropy occurred within tens of µs for samples with complete coverage immersed in 0.1M TBAP:acetonitrile. On the other hand, samples

where the coverage was below 30% showed a constant value of anisotropy up to about 100 µs and a decay at longer timescale. The decay referred to the dye cation absorption showed a slowdown when dye loading was decreased. This finding is consistent with the study reported by Ogawa et al. where the addition of DCA resulted in longer lived photogenerated holes.[29] Data are shown in section 4 of the supporting information.

Analogous measurements for D131:DCA sensitized TiO_2 films with no supporting electrolyte showed much slower anisotropy decays. The samples with full dye coverage showed finite values of anisotropy up to milliseconds. Moreover, decay in anisotropy was much slower in samples with a low dye coverage (see figure 2d).

In order to interpret this set of data, we need to consider some details of the system under study and of the technique used. The measurement of a finite anisotropy in the absorption of the dye cation is due to the fact that the photo-oxidized dye preserves information on the original polarization of the excitation. More precisely, when the sample is pumped with polarized light the population of excited dyes is selected on the basis of their transition dipole moment orientation relative to the pump polarization. Upon electron injection from the dye to the TiO_2 scaffold, the orientation of the transition dipole moment for the dye cation's absorption becomes the relevant physical property for the transient absorption anisotropy measurement. The orientation of the dipole moment of the ground state absorption at the pump excitation wavelength and the orientation of the dye cation dipole moment at the probe beam wavelength are in general different. The relative orientation of the two vectors defines the value of anisotropy measured at early timescales (after electron injection, and structural relaxation of the dye).

A number of different factors could cause the loss in anisotropy for the cation's absorption signal shown in figure 2c-2d. Based on arguments listed below, we conclude that hole transfer between dyes on the surface of the TiO_2 (i) is likely to be the dominant mechanism for anisotropy decay in our observations.

(i) *Hole transfer to other dyes with different dipole moment orientation*. Hole diffusion in the monolayer of dyes on a facet of the TiO_2 could result in loss of anisotropy. The extent to which this happens depends on the degree of disorder of the collection of dyes. In particular, it depends on the orientation of the probed transition dipole moment of the cation and its relation to the geometric configuration of the dyes on the surface. The electrochemical measurements of charge percolation in figure 2a indicate that holes can hop across the edges of the crystals' surface and junctions between particles. This is because the total charge injected in the dyed film during the cyclic voltammetry measurement corresponds to the oxidation of more dyes than are expected on the TiO_2 particles in contact with the FTO. When the individual hole hops across facets, an abrupt variation in its dipole alignment is expected which contributes to the anisotropy decay. Therefore, even if each facet of the nanocrystal were covered by dyes arranged such that the orientation of the relevant dipole moment is conserved, loss in anisotropy would be expected due to hole transfer between different facets of the nanocrystal.

(ii) *Fluctuation in the dyes' conformation*. We have proposed that the movement of dye molecules on the surface of the TiO_2 could explain the high apparent diffusion coefficient observed for the indolene dyes D102 and D149 from electrochemical measurements.[30] We note that the percolation behavior that we observed could be justified by this phenomenon if the movement of D131 could be inhibited by the presence of the coadsorbent DCA. However, we also note that the transient anisotropy would be very unlikely to reach a value of 0 (as we observe in figure 2c-

2d) solely due to fluctuation of dyes' conformation, as the chemical bond to the TiO_2 surface and the presence of the surrounding dyes constrain the set of possible geometrical conformations of the dye on which a hole resides.

(iii) *Desorption of the dyes upon photo-oxidation*. This is unlikely to be a dominant process unless the desorption were inhibited by the presence of the DCA coadsorbents. We see no obvious reason why DCA should hinder D131 desorption on the scale required to explain the observations.

(iv) *Other chemical reactions involving the photo-oxidized dyes* could also result in transient anisotropy decay. This explanation is not consistent with the measurement of long lived signals for the transient absorption of the samples (see figure S6 in the supporting information).

We therefore interpret the features of the transient anisotropy decays of figure 2c and 2d predominantly as a measure of hole transfer between dyes that operates only above the dye loading percolation threshold. Below the percolation threshold, holes are unlikely to reach a different facet from the one where they were generated within the time scale of the measurement since no complete decay in anisotropy is observed. From the increased anisotropy decay time for high dye loading samples in figure 2d relative to 2c we conclude that diffusion of holes appears around 100× slower in air than in the presence of electrolyte. This observation could be explained considering the absence of a polar environment able to screen the dyes from each other. This may result in more distorted configurations of, and poorer coupling to, neighboring dyes in the presence of a dye cation. The presence of a polar electrolyte might also allow articulation of the dyes on the surface, enabling shuttling of charges between dyes.[30]

Dye regeneration by the HTM in solid state DSSCs as a function of pore filling and dye loading

TiO_2 nanocrystalline films sensitized with D131:DCA infiltrated with spiro OMeTAD and the additives LiTFSI and tBP were measured via transient absorption spectroscopy. Figures 3a - 3d show the concentration of holes on D131 dyes and in spiro OMeTAD as a function of time within the µs to 100 µs time scale for a set of devices. These quantities were obtained from the analysis of TAS data measured at 1000 and 1500 nm (the raw data are shown in section 5 of the supporting information) using the technique described in the method section (equation 1). High and low pore filling cases are considered for both full and below 50% D131 coverage. In figure 3a - 3d we also show (right axes) the time dependent regeneration yield calculated using equation 2.

From these graphs we can draw the following observations. Low pore filling results in a significant fraction of holes being left on the dyes at the earliest timescale resolved (~1.5 µs). For the device with full D131 coverage, the regeneration yield at 1.5 µs is higher than for the device with low D131 coverage (0.5 against 0.3). Moreover, for the first sample, we also observe an increase in the hole density in the spiro OMeTAD corresponding to about 20% increase in regeneration yield during the 1 to 100 µs timespan. The final value is higher than the low dye loading case by a factor of more than 2. The low D131 coverage device did not show any increase in the regeneration yield within the measured time window. Samples fabricated with high pore filling showed very high regeneration yield. For the high dye loading case $\eta_{reg} = 1$ (within the error) throughout the timescale of the measurement. However the low dye loading, high pore filling film showed a constant value of $\eta_{reg} = 0.95$. This suggests that for the low dye loading case, even under optimized pore filling conditions, a fraction of holes are left on dye molecules and are not able to reach the HTM. This was not the case when holes were able to percolate on the surface of the TiO_2 in the sample with high dye loading and high pore filling. Indeed, our observations suggest that for the latter case either direct or hole percolation assisted regeneration occurs for all the photo-excited dyes that injected an electron in

the TiO_2. We stress that we neglect any recombination processes that occur at timescales faster than our system resolution (~1 µs) in this analysis. This would decrease the absolute value of the regeneration yield but would not change the observed trends.

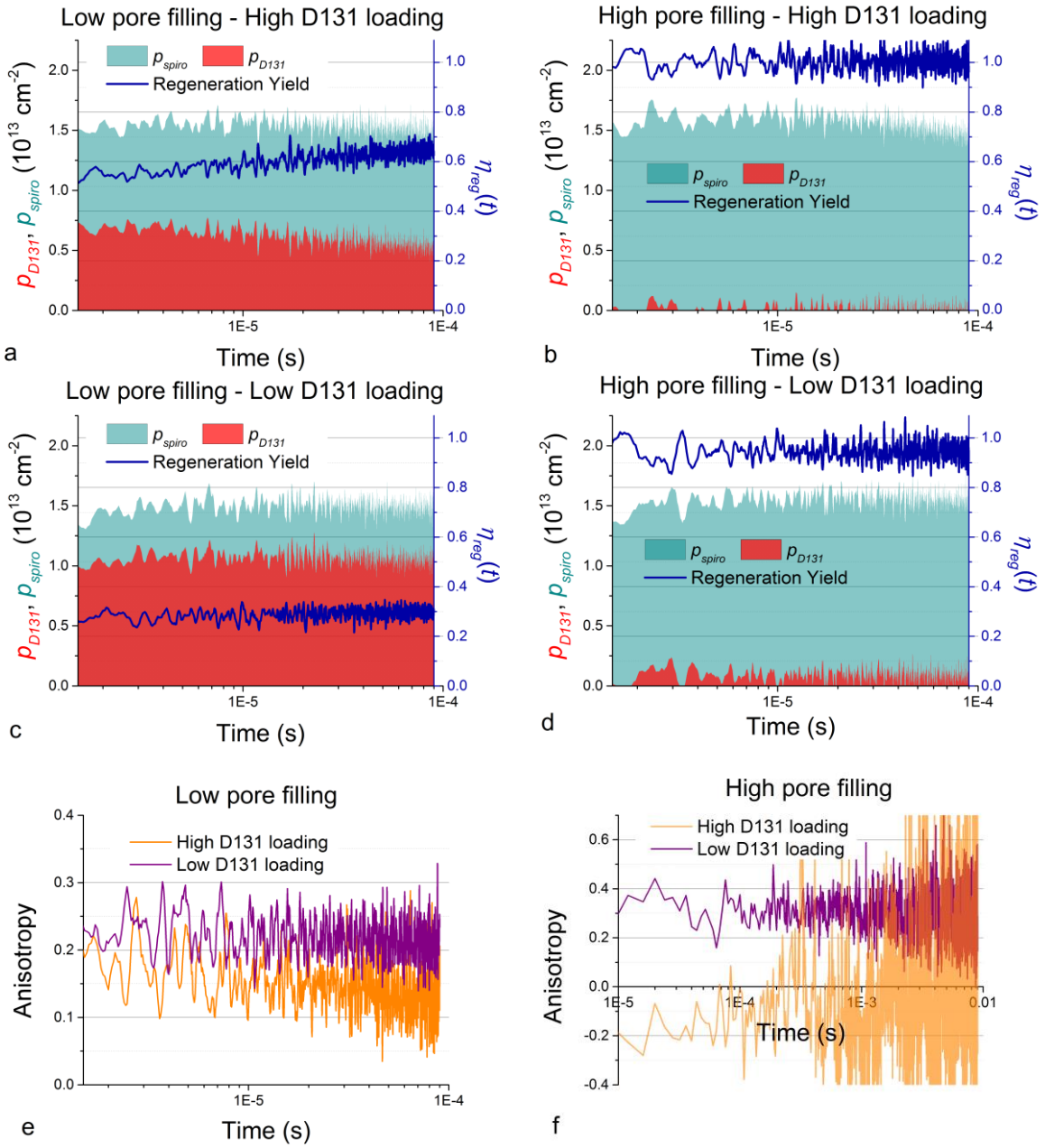

Figure 3. (a-d) Analysis of the kinetics for holes on D131 dyes and on spiro OMeTAD obtained by inverting the linear problem expressed in equation 1 for transient absorption measurements at 1000 and 1500 nm. The left axis displays the hole density dynamics in the dye layer (p_{D131}) and the HTM (p_{spiro}) in the different devices upon laser excitation, whereas the right axis gives an estimate of the time dependent regeneration efficiency ($\eta_{reg}(t)$) of the devices as a function of time (see equation 2). The calculated pore filling fraction and dye loading for the devices were respectively: (a) 3.4%, 88%; (b) 81%, 87%; (c) 3.4%, 35%, (d) 81%, 39%. The methods to evaluate the pore filling and the dye loading are described in section 1 of the supporting information. (e,f) Transient anisotropy, $r(t)$, of the oxidized dye signal, p_{D131}, for the 4 devices analysed in the top 4 figures. Note that the timescale in figure 3f is different from the one used in the other graphs.

To further confirm these findings, transient anisotropy spectroscopy was applied to the same samples. The anisotropy signal related to the holes on the dyes (p_{D131}) was extracted from anisotropy measurements at 1000 nm and by subtracting the spiro OMeTAD contribution at 1000 nm calculated from the signals at 1500 nm. This operation was carried out under the assumption that the absorption tail of the spiro OMeTAD cation at 1000 nm refers to the same dipole moment as the absorption at 1500 nm. In figure 3e and 3f we show the transient anisotropy signal assigned to p_{D131} for the same 4 devices as shown in figure 3a –3d.

From figure 3e, we can detect a drop in anisotropy for the high coverage device, whereas no significant variation can be noted for the low coverage case. Thus for samples with dye loading greater than 50% we observe a simultaneous increase in regeneration yield and drop in anisotropy for the signal related to holes on D131 dyes. This corroborates the hypothesis that hole transport between dyes provides a route for the regeneration of dyes that are not in direct contact with the HTM. The hypothesis is also consistent with the observation that, when low dye loading is considered, both the regeneration yield and the anisotropy profile related to the dye cations population remain constant between 1 and 100 µs. Figure 3f on the other hand gives an interesting insight into the regeneration performance when pore filling is optimized. When the dye loading of the device is low so that percolation of holes through the dyes is prevented, a finite and constant anisotropy signal is detected for p_{D131} up to the 10 ms timescale. This is consistent with a finite fraction of photo-generated holes not being transferred to the HTM from the dye monolayer. On the other hand, no clear anisotropy signal for p_{D131} could be resolved for the device fabricated with high dye loading. This is consistent with the negligible density of holes remaining on the D131 dyes after 1 µs.

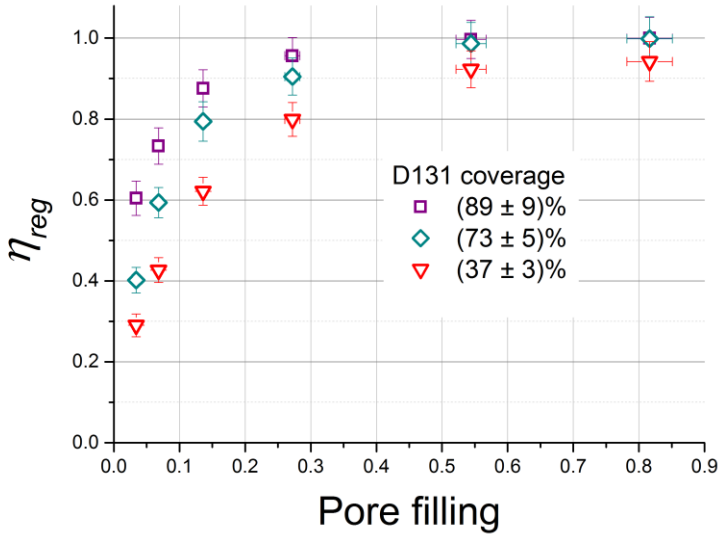

Figure 4. Regeneration efficiency calculated from transient absorption measurements using equation 3 on D131:DCA sensitized TiO_2 films infiltrated with spiro OMeTAD as HTM as a function of pore filling. The experiment has been carried out for three different dye solution compositions to vary the dye coverage.

Transient absorption spectroscopy was carried out on devices fabricated with gradually increasing pore filling fraction and for three different dye solution compositions. The D131:DCA ratios of 1:0, 1:5 and 1:100 were chosen in order to obtain two sets of devices with dye loading above 50% D131 coverage, one with and one without inert coadsorbent, and one with less than 50% D131 coverage. Figure 4 shows the resulting trends of regeneration efficiency (calculated as shown in equation 3) as a function of pore filling for the different dye loading conditions.

The graph shows very clearly that regeneration of the dyes in the architectures investigated here depends significantly on the pore filling of the HTM in the pores of the TiO_2 but also on the dye monolayer composition. The trend suggests that dye regeneration monotonically improves with dye loading. The difference in regeneration yield between the three sets of samples is very evident at low pore filling levels, while it becomes comparable to the experimental error for the high pore filling cases considered. We note that while aggregation of dyes may be beneficial for hole transport in the monolayer, it is generally assumed to reduce the dye excited state lifetime. This can result in lower electron injection and overall photoconversion efficiency of the solar cell.[31,32]

The resolution of the kinetics shown in figure 3 and the quantification of the regeneration yield displayed in figure 4 rely on the knowledge of the extinction coefficient of the oxidized dye and HTM at the probed wavelengths. The values of extinction coefficient used in this work were extracted from electrochemical measurements, in the presence of an electrolyte. We note that such values can vary when considering different environments. The relative trend which we discuss here between different samples should however remain valid.

Devices fabricated without the additives LiTFSI and tBP show faster diffusion of holes in the dye monolayer and result in remarkably higher regeneration yield under low pore filling conditions (see section 6 of the supporting information). We note that the latter effect is observed for all dye loadings investigated here, including samples with dye surface coverage below 40%. When the concentration of additives is decreased for the high pore filling case, we observe that 100% regeneration yield can be obtained also for dye surface coverage below percolation. These results suggest that the presence of LiTFSI and/or tBP slowdown hole diffusion in the dye monolayer. This has a negative impact on regeneration.

In section 7 of the supporting information we show the effect of varying the dye loading and the HTM pore filling on the short circuit current of full solid state DSSC devices using the dye D149. The results are consistent with hole transport between dyes contributing to the photocurrent generation under low HTM pore filling conditions.

These results suggest that a significant fraction of the dyes contributing to light absorption in a solid state DSSC undergo “slow” (from µs up to hundreds of µs depending on the pore filling) regeneration. This implies that upon photoexcitation, such molecules can spend relatively long time in the oxidized state. This observation emphasizes the need for more investigation of molecular structures which show highly stable cationic state.[33]

Hole diffusion as a probe of the surrounding environment: HTM film formation

From the above discussion, we conclude that in a solid state DSSC device, a decrease in dye loading results in decreased regeneration yield. The results also suggest that this trend is related to the ability of holes to diffuse within the dye monolayer. If one assumes that when the dye loading is below the percolation threshold, hole transfer between dyes at the nanoscale is negligible (as indicated by the results in figure 2d), then the only dyes that can be regenerated are those that are in contact with the HTM. This implies that the regeneration yield in this architecture type would be a close estimate of the fraction of the dyed TiO_2 surface covered by the HTM in the device. Above the dye percolation threshold, this concept should not be valid, given the contribution of hole transfer between dyes to the regeneration yield discussed in the previous sections.

If we assume, based on observations outlined in section 8 in the supporting information, that the morphology of the HTM in the pores is not influenced by dye loading then we can use the results in figure 4 to infer information about the fraction of the dyed TiO_2 surface covered by the HTM. Figure 5a shows the regeneration yield data from figure 4 plotted versus the dyed TiO_2 surface fraction covered by the HTM assuming that the latter is equal to the regeneration yield for the case of low

dye loading, $\eta_{reg,low\ loading}$. It is apparent that the relationship between the fraction of the dyed TiO_2 surface covered by HTM and regeneration yield for the systems where the dye loading is above the percolation threshold is not linear.

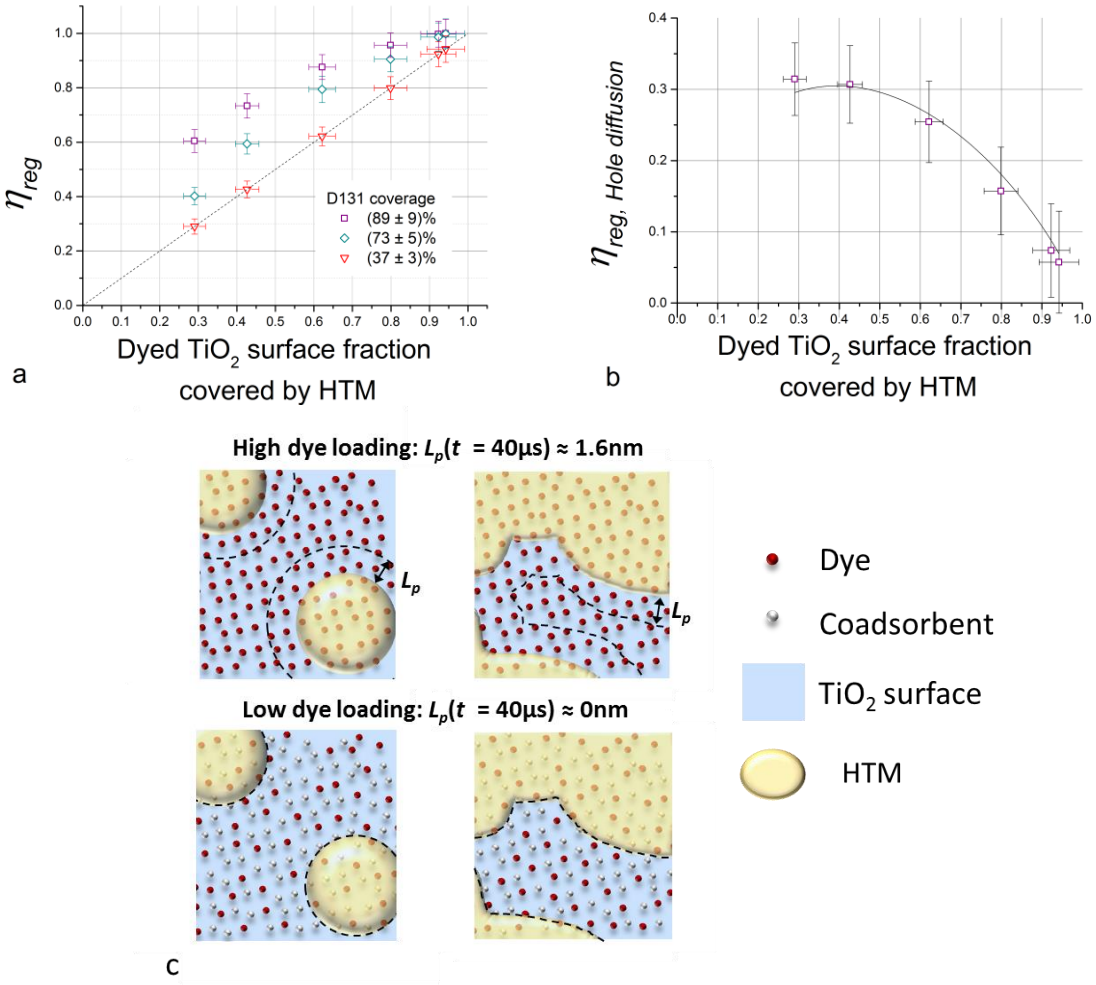

Figure 5. (a) Regeneration efficiency (from figure 4) plotted as function of dyed TiO_2 surface fraction covered by the HTM spiro OMeTAD. The latter is considered to be equal to the regeneration yield at low dye loading conditions (dashed line in figure 5a). (b) Component of regeneration yield that can be ascribed to hole diffusion in the dye monolayer for the high dye loading case. (c) This quantity can be approximated as the fraction of the dyed TiO_2 surface corresponding to the area conformal to the perimeter of the HTM islands with thickness L_p shown in the schematic. L_p is an estimate of the distance covered by the holes in the dye monolayer within 40 µs from photogeneration (see section 9 in the supporting information). The solid line in figure 5b is the fit of the expression for this surface fraction (HTM perimeter × L_p) as a function of HTM coverage to the data.

Given the above model, we calculate the regeneration yield due to hole diffusion between dyes ($\eta_{reg,holediff}$). This is the fraction of holes that reached the spiro OMeTAD phase through transport in the dye monolayer, always assuming that such phenomenon does not occur to a significant extent in the case of low coverage. Therefore:

$$\eta_{reg,holediff} = \eta_{reg} - \eta_{reg,lowloading} \qquad \text{Eq. 5}$$

where η_{reg} is the total regeneration yield and $\eta_{reg,lowloading}$ is the total regeneration yield for the low dye loading case. The trend in regeneration due to hole diffusion in the dye monolayer observed refers to the specific morphology of the "islands" of HTM in contact with the sensitized surface. Therefore, assuming a known hole transport regime in the dye monolayer one could extract information about the HTM film morphology or *vice versa*. We interpret $\eta_{reg,holediff}$ as the fraction of the dyed surface which is uncovered by HTM and from which regeneration assisted by hole percolation is possible. We can approximate this area as the product of the HTM islands' perimeter P and the distance travelled by the holes in the uncovered monolayer of dyes L_p as shown in figure 5c. L_p can be calculated as $(D_{2D}\ t_d)^{0.5}$ (where D_{2D} is the holes diffusion coefficient on the surface of the TiO_2 and t_d is the time during which the holes have diffused). P is a function of the dyed TiO_2 surface covered by the HTM. In particular, for a constant density of, randomly distributed, simultaneous surface nucleation centers, an analytical solution to the problem has been demonstrated.[34] The perimeter of HTM in contact with the dyed TiO_2 per unit surface area P' can be expressed as:

$$P'(C) = (1-C)\sqrt{4\pi N \ln\left(\frac{1}{1-C}\right)} \qquad \text{Eq. 6}$$

where C is the dyed TiO_2 surface fraction covered by the HTM and N is the density of nucleation centres (cm^{-2}).

Figure 5b displays the plot of $\eta_{reg,holediff}$ against dyed TiO_2 surface coverage by the HTM for the set of samples with complete dye loading. The fit to the data corresponds to the expected trend of the product $L_p \times P'$ assuming a constant density of randomly distributed nucleation centers on the surface for all the different spiro OMeTAD concentrations considered. The only fitting parameter used is the product $L_p \times N^{1/2}$ and is equal to 0.20. The value of L_p could in principle be estimated from measurements of anisotropy decay. We note that L_p is likely to vary due to different pore filling conditions and potentially with different amount of additives present on the surface. A value in the order of 1.55 nm for L_p (see section 9 in the supporting information for this estimate) would result in a nucleation centre density value of 1.66×10^{12} cm^{-2}. This corresponds to 1 nucleation center every 8^2 nm^2 which is in the same order of magnitude as the surface area of a TiO_2 particle facet. The implication is that growth of the spiro OMeTAD film occurs starting from a nucleation point density that is comparable to the density of TiO_2 particles' facets. This would therefore imply that the morphology of the HTM in the pores is as coarse as the nano-morphology of the TiO_2 scaffold, resulting in few but relatively large areas of dyed TiO_2 being uncovered. Despite the good quality of the fit shown in figure 5b, a different nucleation growth behavior may be expected for different concentrations of the spiro OMeTAD solution. Also, this analysis assumes homogeneous hole transport properties in the dye monolayer. We note that the anisotropy decays in figure 2 show highly dispersive character which suggests that describing holes migration across the particle's surface with a basic diffusion model is an oversimplification. Figure 5a shows that, for the high dye loading case, regeneration reaches values close to unity at a minimum surface coverage by the HTM of about 80 to 90%. We can conclude that this is consistent with two possible scenarios: a coarse distribution of HTM (on a pore to pore scale as described by the model above) and/or a dye monolayer showing high degree of disorder. Inhomogeneous coverage by the HTM (specifically, non-uniform filling of the pores) would be expected if the ability of the HTM to infiltrate in the dyed mesostructure were a function of the pore size. Also, the presence of air bubble in the pores during the HTM spin coating process could lead to specific regions of the film not being filled by the HTM. SEM analysis of pore filling and HTM film morphology has previously been reported. [35,36,5] However, SEM is a surface analysis technique and has some limitations for inferring bulk properties (even in the cross sectional case, samples need to be cut or cleaved in order to expose an "internal" surface to the measurement). Given the relationship between hole percolation assisted regeneration and HTM morphology, our analysis represents a useful non-invasive, contact-less, technique to

investigate the interfacial properties in the bulk of solid state dye sensitized devices. We note that hole percolation on sensitized surfaces could be used as a "probe" to study the surrounding local environment in other systems. Finally, our analysis of holes diffusing in molecular monolayers and being transferred to the HTM is relevant to solar fuel devices. In these photo-electrochemical systems, intermolecular charge transfer between surface sensitizers can be used to funnel charges to catalysts to, for example, drive multi-electron reactions.[15,37,38]

Conclusions

We investigated the mechanism of dye regeneration in the photoconversion process of solid state DSSCs. We showed that the regeneration yield of devices using the dye D131 and the hole transporting material spiro OMeTAD increases with the pore filling of the dyed mesostructure by the HTM, consistently with previous reports for different dyes, but also increases with the dye surface coverage. Furthermore, we related the hole diffusion in the dye monolayer probed with different techniques to the dye loading and present a multiscale description of the percolation process. This resulted in the deconvolution of the contribution of dyes which are left uncovered from the one of dyes in contact with the HTM phase to the measured regeneration yield of the solar cell. Our analysis demonstrated the role of inter-dye hole transport to be an important part of the working principle of this class of devices. Developing new strategies to characterize charge diffusion in molecular monolayers can lead to a deeper understanding of devices including sensitized oxide nanostructures. In this study, we showed the example of using holes on dyes to explore the nanomorphology of the environment resulting from the solution processing of the HTM in the dyed TiO_2 mesostructure.

Acknowledgements

We thank Shane Ardo and Gerard J. Meyer for useful discussion. DM and PB are grateful for EPSRC fellowship EP/J002305/1.

Supporting Information Available

The supporting information contains a detailed description of the experimental method for sample preparation, dye loading and HTM pore filling quantification. It illustrates the spectroelectrochemical measurement of the oxidized D131 absorption spectrum and extinction coefficient. In the supporting information we also discuss dye loading uniformity, photogenerated hole lifietime and include the raw transient absorption spectroscopy data used to calculate the time dependent regeneration yield displayed in Figure 3. In addition, the document shows the effect of the additives LiTFSI and tBP on the dye regeneration yield as well as the pore filling and dye loading dependence of solid state DSSCs' photocurrent. Finally, we discuss dyed TiO_2 surface wetting and the quantification of hole diffusion in the D131 monolayers in solar cell devices. This information is available free of charge via the Internet at http://pubs.acs.org.

References

(1) O'Regan, B. C.; Grätzel, M. A Low-Cost High Efficiency Solar Cell Based on Dye-Sensitized Colloidal TiO2 Films. *Nature* **1991**, *353*, 737.

(2) Hagfeldt, A.; Gratzel, M. Light-Induced Redox Reactions in Nanocrystalline Systems. *Chem. Rev.* **1995**, *95*, 49–68.

(3) Bach, U.; Lupo, D.; Comte, P.; Moser, J. E.; Weissoertel, F.; Salbeck, J.; Spreizer, H.; Grätzel, M. Solid-State Dye-Sensitized Mesoporous TiO2 Solar Cells with High Photon-to-Electron Conversion Efficiencies. *Nature* **1998**, *395*, 583–585.

(4) Docampo, P.; Hey, A.; Guldin, S.; Gunning, R.; Steiner, U.; Snaith, H. J. Pore Filling of Spiro-OMeTAD in Solid-State Dye-Sensitized Solar Cells Determined Via Optical Reflectometry. *Adv. Funct. Mater.* **2012**, *22*, 5010–5019.

(5) Cappel, U. B.; Gibson, E. a.; Hagfeldt, A.; Boschloo, G. Dye Regeneration by Spiro-MeOTAD in Solid State Dye-Sensitized Solar Cells Studied by Photoinduced Absorption Spectroscopy and Spectroelectrochemistry. *J. Phys. Chem. C* **2009**, *113*, 6275–6281.

(6) Haque, S. a; Park, T.; Holmes, A. B.; Durrant, J. R. Transient Optical Studies of Interfacial Energetic Disorder at Nanostructured Dye-Sensitised Inorganic/organic Semiconductor Heterojunctions. *Chemphyschem* **2003**, *4*, 89–93.

(7) Kroeze, J. E.; Hirata, N.; Schmidt-Mende, L.; Orizu, C.; Ogier, S. D.; Carr, K.; Grätzel, M.; Durrant, J. R. Parameters Influencing Charge Separation in Solid-State Dye-Sensitized Solar Cells Using Novel Hole Conductors. *Adv. Funct. Mater.* **2006**, *16*, 1832–1838.

(8) Melas-Kyriazi, J.; Ding, I.-K.; Marchioro, A.; Punzi, A.; Hardin, B. E.; Burkhard, G. F.; Tétreault, N.; Grätzel, M.; Moser, J.-E.; McGehee, M. D. The Effect of Hole Transport Material Pore Filling on Photovoltaic Performance in Solid-State Dye-Sensitized Solar Cells. *Adv. Energy Mater.* **2011**, *1* (3), 407–414.

(9) Weisspfennig, C. T.; Hollman, D. J.; Menelaou, C.; Stranks, S. D.; Joyce, H. J.; Johnston, M. B.; Snaith, H. J.; Herz, L. M. Dependence of Dye Regeneration and Charge Collection on the Pore-Filling Fraction in Solid-State Dye-Sensitized Solar Cells. *Adv. Funct. Mater.* **2013**, *24*, 668–677.

(10) Heimer, T. A.; Arcangelis, S. T. D.; Farzad, F.; Stipkala, J. M.; Meyer, G. J. An Acetylacetonate-Based Semiconductor - Sensitizer Linkage. *Inorg. Chem.* **1996**, *1669*, 5319–5324.

(11) Bonhôte, P.; Gogniat, E.; Tingry, S.; Barbe, C.; Vlachopoulos, N.; Lenzmann, F.; Comte, P.; Grätzel, M. Efficient Lateral Electron Transport inside a Monolayer of Aromatic Amines Anchored on Nanocrystalline Metal Oxide Films. *J. Phys. Chem. B* **1998**, *5647*, 1498–1507.

(12) Wang, Q.; Zakeeruddin, S. M.; Nazeeruddin, M. K.; Humphry-Baker, R.; Grätzel, M. Molecular Wiring of Nanocrystals: NCS-Enhanced Cross-Surface Charge Transfer in Self-Assembled Ru-Complex Monolayer on Mesoscopic Oxide Films. *J. Am. Chem. Soc.* **2006**, *128*, 4446–4452.

(13) Fattori, A.; Peter, L. M.; Wang, H.; Miura, H.; Marken, F. Fast Hole Surface Conduction Observed for Indoline Sensitizer Dyes Immobilized at Fluorine-Doped Tin Oxide - TiO 2 Surfaces. *J. Phys. Chem. C* **2010**, *205*, 11822–11828.

(14) Westermark, K.; Tingry, S.; Persson, P.; Rensmo, H.; Lunell, S.; Hagfeldt, A.; Siegbahn, H. Triarylamine on Nanocrystalline TiO 2 Studied in Its Reduced and Oxidized State by Photoelectron Spectroscopy. *J. Phys. Chem. B* **2001**, *105*, 7182–7187.

(15) Ardo, S.; Meyer, G. J. Direct Observation of Photodriven Intermolecular Hole Transfer across TiO2 Nanocrystallites: Lateral Self-Exchange Reactions and Catalyst Oxidation. *J. Am. Chem. Soc.* **2010**, *132*, 9283–9285.

(16) Moia, D.; Leijtens, T.; Noel, N.; Snaith, H. J.; Nelson, J.; Barnes, P. R. F. Dye Monolayers Used as Hole Transporting Medium in Dye Sensitized Solar Cells. Accepted in *Adv. Mater.*

(17) Bach, U.; Tachibana, Y.; Moser, J.; Haque, S. A.; Durrant, J. R.; Grätzel, M. Charge Separation in Solid-State Dye-Sensitized Heterojunction Solar Cells. *J. Am. Chem. Soc.* **1999**, *2*, 7445–7446.

(18) Boschloo, G.; Marinado, T.; Nonomura, K.; Edvinsson, T.; Agrios, A. G.; Hagberg, D. P.; Sun, L.; Quintana, M.; Karthikeyan, C. S.; Thelakkat, M.; et al. A Comparative Study of a Polyene-Diphenylaniline Dye and Ru(dcbpy)2(NCS)2 in Electrolyte-Based and Solid-State Dye-Sensitized Solar Cells. *Thin Solid Films* **2008**, *516*, 7214–7217.

(19) Moia, D.; Vaissier, V.; López-Duarte, I.; Torres, T.; Nazeeruddin, M. K.; O'Regan, B. C.; Nelson, J.; Barnes, P. R. F. The Reorganization Energy of Intermolecular Hole Hopping between Dyes Anchored to Surfaces. *Chem. Sci.* **2014**, *5*, 281-290.

(20) Yang, L.; Cappel, U. B.; Unger, E. L.; Karlsson, M.; Karlsson, K. M.; Gabrielsson, E.; Sun, L.; Boschloo, G.; Hagfeldt, A.; Johansson, E. M. J. Comparing Spiro-OMeTAD and P3HT Hole Conductors in Efficient Solid State Dye-Sensitized Solar Cells. *Phys. Chem. Chem. Phys.* **2012**, *14*, 779–789.

(21) Anderson, A. Y.; Barnes, P. R. F.; Durrant, J. R.; O'Regan, B. C. Quantifying Regeneration in Dye-Sensitized Solar Cells. *J. Phys. Chem. C* **2011**, *115*, 2439–2447.

(22) Anderson, A. Y.; Barnes, P. R. F.; Durrant, J. R.; O'Regan, B. C. Simultaneous Transient Absorption and Transient Electrical Measurements on Operating Dye-Sensitized Solar Cells : Elucidating the Intermediates in Iodide Oxidation. *J. Phys. Chem. C* **2010**, *114*, 1953–1958.

(23) Berger, T.; Anta, J. A.; Morales-Flórez, V. Electrons in the Band Gap : Spectroscopic Characterization of Anatase TiO 2 Nanocrystal Electrodes under Fermi Level Control. *J. Phys. Chem. C* **2012**, *116*, 11444–11455.

(24) Cappel, U. B.; Daeneke, T.; Bach, U. Oxygen-Induced Doping of Spiro-MeOTAD in Solid-State Dye-Sensitized Solar Cells and Its Impact on Device Performance. *Nano Lett.* **2012**, *12*, 4925–4931.

(25) Lakowicz, J. R. *Principles of Fluorescence Spectroscopy*, 3rd ed.; Springer Science + Business Media: New York, 2006.

(26) Zhang, W.; Zhu, R.; Li, F.; Wang, Q.; Liu, B. High-Performance Solid-State Organic Dye Sensitized Solar Cells with P3HT as Hole Transporter. *J. Phys. Chem. C* **2011**, *115*, 7038–7043.

(27) O'Regan, B.; Li, X.; Ghaddar, T. Dye Adsorption, Desorption, and Distribution in Mesoporous TiO2 Films, and Its Effects on Recombination Losses in Dye Sensitized Solar Cells. *Energy Environ. Sci.* **2012**, *5*, 7203-7215.

(28) Li, X.; Nazeeruddin, M. K.; Thelakkat, M.; Barnes, P. R. F.; Vilar, R.; Durrant, J. R. Spectroelectrochemical Studies of Hole Percolation on Functionalised Nanocrystalline TiO2 Films: A Comparison of Two Different Ruthenium Complexes. *Phys. Chem. Chem. Phys.* **2011**, *13*, 1575–1584.

(29) Ogawa, J.; Koumura, N.; Hara, K.; Mori, S. Deceleration of Dye Cation Reduction Kinetics by Adding Alkyl Chains to the Π-Conjugated Linker of Dye Molecules. *Jpn. J. Appl. Phys.* **2014**, *53*, 1–5.

(30) Vaissier, V.; Mosconi, E.; Moia, D.; Pastore, M.; Frost, J. M.; De Angelis, F.; Barnes, P. R. F.; Nelson, J. Effect of Molecular Fluctuations on Hole Diffusion within Dye Monolayers. *Chem. Mater.* **2014**, *26*, 4731–4740.

(31) De Miguel, G.; Marchena, M.; Ziółek, M.; Pandey, S. S.; Hayase, S.; Douhal, a. Femto- to Millisecond Photophysical Characterization of Indole-Based Squaraines Adsorbed on TiO 2 Nanoparticle Thin Films. *J. Phys. Chem. C* **2012**, *116*, 12137–12148.

(32) Matsuzaki, H.; Murakami, T. N.; Masaki, N.; Furube, A.; Kimura, M.; Mori, S. Dye Aggregation Effect on Interfacial Electron-Transfer Dynamics in Zinc Phthalocyanine-Sensitized Solar Cells. *J. Phys. Chem. C* **2014**, *118*, 17205–17212.

(33) Katoh, R.; Furube, A.; Mori, S.; Miyashita, M.; Sunahara, K.; Koumura, N.; Hara, K. Highly Stable Sensitizer Dyes for Dye-Sensitized Solar Cells: Role of the Oligothiophene Moiety. *Energy Environ. Sci.* **2009**, *2*, 542–546.

(34) Tomellini, M.; Fanfoni, M. Kinetics of the Total Cluster Perimeter in Thin Film Nucleation on Solid Surfaces. *Surf. Sci.* **1996**, *349*, L191–L198.

(35) Schmidt-Mende, L.; Grätzel, M. TiO2 Pore-Filling and Its Effect on the Efficiency of Solid-State Dye-Sensitized Solar Cells. *Thin Solid Films* **2006**, *500*, 296–301.

(36) Snaith, H. J.; Humphry-Baker, R.; Chen, P.; Cesar, I.; Zakeeruddin, S. M.; Grätzel, M. Charge Collection and Pore Filling in Solid-State Dye-Sensitized Solar Cells. *Nanotechnology* **2008**, *19*, 424003.

(37) Swierk, J. R.; Méndez-Hernández, D. D.; McCool, N. S.; Liddell, P.; Terazono, Y.; Pahk, I.; Tomlin, J. J.; Oster, N. V.; Moore, T. a.; Moore, A. L.; et al. Metal-Free Organic Sensitizers for Use in Water-Splitting Dye-Sensitized Photoelectrochemical Cells. *Proc. Natl. Acad. Sci.* **2015**, *112*, 1681–1686.

(38) Brennan, B. J.; Durrell, A. C.; Koepf, M.; Crabtree, R. H.; Brudvig, G. W. Towards Multielectron Photocatalysis: A Porphyrin Array for Lateral Hole Transfer and Capture on a Metal Oxide Surface. *Phys. Chem. Chem. Phys.* **2015**, *17*, 12728–12734.

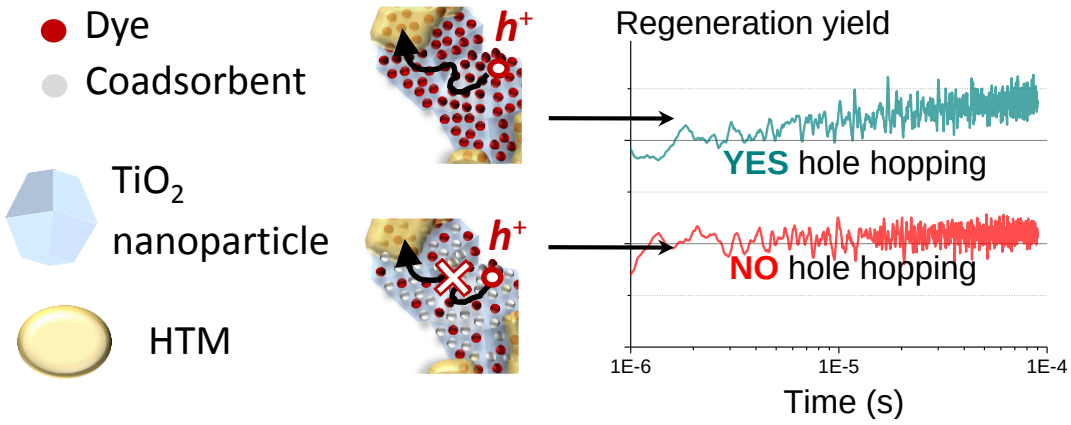

Table of Content